Available online at www.sciencedirect.com
SCIENCE DIRECT®
Journal of the European Ceramic Society 25 (2005) 2313–2317
www.elsevier.com/locate/jeurceramsoc

Optical studies of $0.65PbMg_{1/3}Nb_{2/3}O_3$–$0.35PbTiO_3$ thin films

K.Y. Chan, W.S. Tsang, C.L. Mak*, K.H. Wong

Department of Applied Physics, The Hong Kong Polytechnic University, Hung Hom, Hong Kong, China

Available online 28 March 2005

Abstract

$0.65PbMg_{1/3}Nb_{2/3}O_3$–$0.35PbTiO_3$ (PMN–PT) thin films with different deposition temperatures were fabricated on (0 0 1)MgO single crystal substrates using pulsed laser deposition (PLD). X-ray diffraction (XRD) showed that the films are epitaxially grown on (0 0 1)MgO substrates. Spectroscopic ellipsometer (SE) was used to characterize the optical properties including refractive indices as well as extinction coefficients of these PMN–PT films in energy range of 0.75–3.5 eV. By fitting the measured ellipsometeric spectra, film thicknesses, surface roughness and optical properties were derived for all PMN–PT films. The film thickness and surface roughness obtained by SE were consistent with those measured by scanning electron microscopy (SEM) and atomic force microscopy (AFM) respectively. The optical band gap energies of PMN–PT films were deduced from the obtained extinction coefficients using Tauc equation. These values were comparable to those obtained by optical transmittance measurements. Our analysis revealed that the optimum refractive index emerges as the film fabricated at ∼670 °C.

Keywords: Optical properties; Titanates; Films; Pulsed laser deposition

1. Introduction

The good electro-optic properties of ferroelectrics coupled with the advances made recently in thin film fabrication technology allow thin-film ferroelectrics to be considered as a formidable candidate for many integrated optic devices. Potential applications include low-voltage electro-optic switches, compact low-threshold gain devices and second harmonic generators.[1] Among various ferroelectrics for optical applications, $0.65PbMg_{1/3}Nb_{2/3}O_3$–$0.35PbTiO_3$ (PMN–PT) is one of the most promising ferroelectric candidates due to its extremely high electro-optic coefficient and strong photorefractive effect.[2] Indeed, PMN–PT has an electro-optic coefficient larger than the best value reported for $(Pb,La)(Zr,Ti)O_3$ thin films.[3]

In this paper, we report the changes of refractive indices and extinction coefficients of PMN–PT films as a function of fabrication temperature. PMN–PT films were grown on MgO single crystal using pulsed laser deposition (PLD) method. The choice of using MgO substrate is based on the small lattice mismatch and large difference in refractive index between PMN–PT film and MgO substrate. MgO single crystal has a lattice constant of 4.21 Å which is close to that of PMN–PT (4.02 Å).[4,5] The refractive index of 0.7PMN–0.3PT ceramics is 2.598 at 633 nm,[2] and this value is much larger than that of MgO single crystal (1.734) at 650 nm.[6] A larger refractive index difference between the film and substrate increases the amplitude of oscillations of ellipsometric spectra, and thus enhances the accuracy of ellipsometric measurements. After obtaining the extinction coefficients of PMN–PT films, the absorption coefficients, and hence the band gap energies of these films were estimated. Such band gap values were compared to those values measured by optical transmittance measurements. Good agreement was found between the two sets of data. Finally, the effects of deposition temperature on the optical properties as well as the band gap energies of PMN–PT films were discussed.

2. Experiment

PMN–PT films were grown on (0 0 1)MgO single crystal substrates by PLD using an ArF excimer-laser. Three different deposition temperatures of 630, 670 and 710 °C were employed in our experiment. The 25-mm diameter and 5-mm

* Corresponding author. Tel.: +852 2766 5669; fax: +852 2333 7629.
E-mail address: apaclmak@polyu.edu.hk (C.L. Mak).

0955-2219/$ – see front matter © 2005 Elsevier Ltd. All rights reserved.
doi:10.1016/j.jeurceramsoc.2005.03.063

thick cylindrical PMN–PT target was homemade from single-phase powder pressed at 80 MPa and sintered at 900 °C for 10 h. Unless stated otherwise, the following conditions for the deposition of PMN–PT films were employed in all cases. The PMN–PT films were deposited in a high vacuum chamber equipped with a rotating holder. The distance between the substrate and the target was kept at 5 cm throughout the experiment. The laser was operated at an energy density of 4 J/cm^2 and a repetition rate of 6 Hz. The ambient oxygen pressure was 200 mTorr and the deposition time was 20 min. After deposition, the as-grown PMN–PT films were post-annealed at the deposition temperature and pressure for another 10 min. Afterwards, the films were cooled naturally to room temperature. X-ray diffraction (XRD, Philip PW3710) using Cu Kα radiation, scanning electron microscopy (SEM, Leico, Stereoscan440) and atomic force microscopy (AFM) were employed to characterize the structural properties of the PMN–PT films. For optical analyses, spectroellipsometry (SE) were carried out by a spectroscopic phase modulated ellipsometer (Jobin Yvon UVISEL) at photon energy between 0.75 and 3.5 eV with 0.01 eV intervals. An incident angle of 70° was used throughout our measurements. Finally, optical transmittance measurement was carried out by a two-beam spectrophotometer (Shimadzu UV-2101).

3. Results and discussion

The XRD $\theta - 2\theta$ profiles of the PMN–PT/MgO films with different deposition temperatures are shown in Fig. 1. Highly oriented PMN–PT films of perovskite phase are observed. The out-of-plane lattice constants calculated from the diffraction angles of (0 0 2) peak with deposition temperatures of 630, 670 and 710 °C were 3.99, 4.02 and 4.02 Å, respectively. The full-width half-maximum (FWHM) of the rocking curves for the PMN–PT films were 1.65, 0.79 and 2.3°, respectively. To give an idea of the instrumentation limit of our XRD machine, the FWHM value for MgO substrate is ≤0.2°. XRD ϕ-scans of the (2 0 2)PMN–PT and (2 0 2)MgO were performed to confirm the epitaxy of our films. Inset of Fig. 1 shows a typical ϕ-scan for PMN–PT film deposited at 670 °C. The peaks of PMN–PT and MgO are at the same position and separated by 90°. This clearly shows the four-folded symmetry of both the film and the substrate. On the basis of our XRD results, it is concluded that all PMN–PT films are cube-on-cube grown on (0 0 1)MgO substrates with an in-plane epitaxial relationship of (0 0 1)PMN–PT || (0 0 1)MgO.

The surface and cross-section SEM images of PMN–PT films deposited at 630, 670 and 710 °C were measured. In general, the surfaces are smooth and crack-free for films deposited at 630 and 670 °C, while the surface is slightly rougher for film deposited at 710 °C. According to our cross-section SEM images, the film and the substrate are easily distinguished for all samples. Fig. 2 shows the SEM images of PMN–PT film deposited at 670 °C. Here, thickness of the film and the root-mean-square (rms) roughness were found

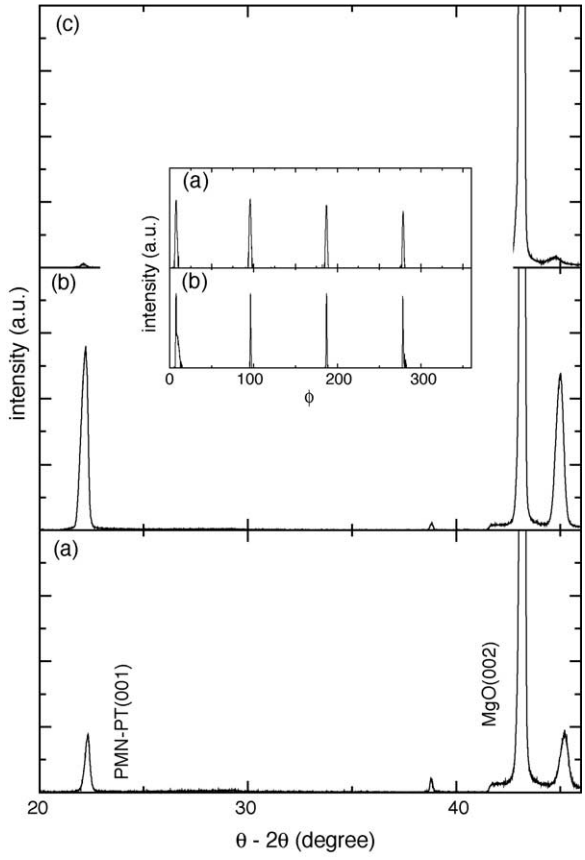

Fig. 1. X-ray diffraction patterns of PMN–PT films deposited at: (a) 630 °C; (b) 670 °C; and (c) 710 °C grown on MgO substrates. Inset shows the XRD ϕ scans of the (a) PMN–PT(202) and (b) MgO(202) with deposition temperature 670 °C.

to be ∼561 and ∼3.9 nm, respectively. These values are very close to those obtained by SE (Table 1). Indeed, all films have very similar features.

Fig. 3 shows the ellipsometric spectra of experimental and simulated ellipsometric parameters, I_S and I_C, for PMN–PT film deposited at 710 °C. Generally speaking, SE measures the traditional ellipsometric angles, ψ and Δ, as functions of photon energy in the experiment. However, spectroscopic phase modulated method was used in our study. In this method, the measuring parameters were I_S and I_C instead of ψ and Δ. The details can be found in elsewhere.[7,8]

The optical properties of oxygen–octahedral ferroelectrics are usually dominated by the BO_6 octahedra, which governs the low lying conduction bands and the highest valence bands. This lowest energy oscillator is the largest contributor to the

Table 1
The physical parameters for different PMN–PT films obtained by SE, SEM and AFM

Deposition temperature (°C)	d_1 (nm)	d_2 (nm)	SEM $d = d_1 + d_2$ (nm)	AFM d_2 (nm)
630	536	2.5	470	4.3
670	538	3.2	561	3.9
710	437	6.6	436	5.5

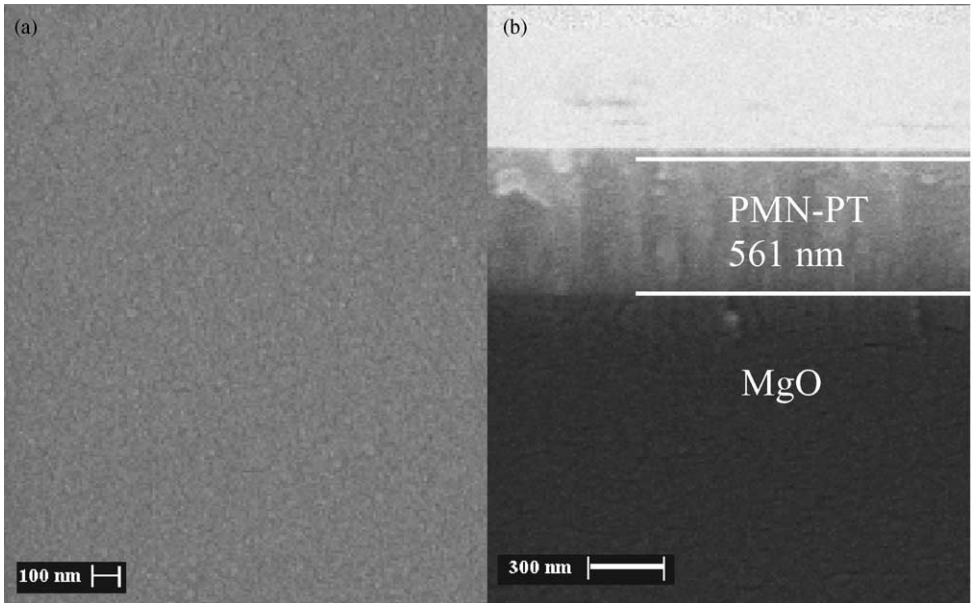

Fig. 2. SEM micrographs show the (a) surface morphology and (b) cross-section of PMN–PT film deposited at 670 °C.

dispersion of the refractive index. Other ions in the structure contribute to the higher-lying conduction band and have a small effect on the optical properties of these ferroelectrics. Hence, a Lorentz oscillator model of the dielectric function with three oscillators,

$$\varepsilon(\omega) = \varepsilon_\infty + \sum_{j=1}^{3} \frac{f_j \omega_{oj}^2}{\omega_{oj}^2 - \omega^2 + i\gamma_j \omega} \quad (1)$$

was used to describe the dominated interband oscillator of PMN–PT. The parameters ε_∞, f_j, $\omega_o$and γ_j are the contributions of high-energy excitations, oscillator weightings, resonance energies and half widths, respectively. In our fitting, the refractive index of the substrate was obtained from MgO single crystal.[6] Our initial analysis was based on a single-layer Lorentz model. Poor agreement, however, was obtained with the experimental data. In subsequent analysis, we modified the single-layer Lorentz model into a double-layer Lorentz model (inset of Fig. 3). In this model, we assume that the films consist of two layers – a bottom bulk PMN–PT layer and a surface layer that composed of bulk PMN–PT as well as voids. These voids in the surface layer were mainly caused by surface roughness. Here, f_{v2} refers to the volume percentage of air in the surface layer. The net optical constants of the mixed layer (PMN–PT + void) were calculated using Bruggeman effective medium approximation. Based on this double-layer Lorentz model, we analyzed the data over the spectra range 0.75–3.5 eV. Good fits between the simulated values of I_S as well as I_C and the experimental data were obtained. The solid lines in Fig. 3 denote these fitted results. Table 1 lists the layer thicknesses of all PMN–PT films obtained from the double-layer Lorentz model, SEM and AFM measurements.

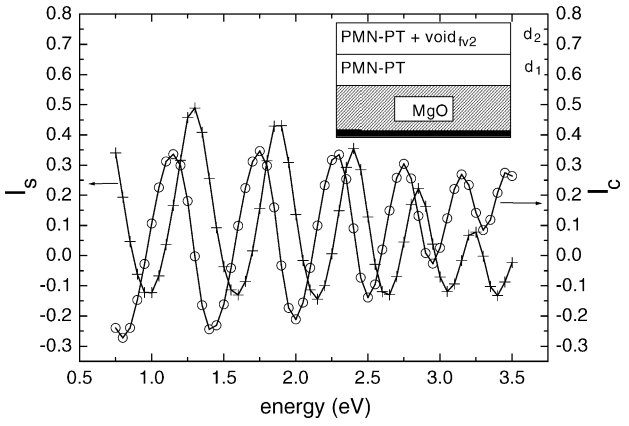

Fig. 3. Spectra of the ellipsometric parameters I_S and I_C as functions of photon energy from PMN–PT films deposited 670 °C. The (+) and (◯) are the measured I_S and I_C values, respectively, while the solid lines are model fitting. Inset shows the schematic picture of the double-layer Lorentz model.

Fig. 4 shows the refractive index dispersion curves of PMN–PT films deposited at different temperatures based on Eq. (1). In general, the refractive index n appears to be continuously increased nonlinearly over the whole energy range from 0.75 to 3.5 eV. Indeed, it increases more sensitively at higher energies. The extinction coefficient k, on the other hand, is fairly flat below 2.5 eV. This behavior is typical of an insulator or semiconductor in the range of energy near the band gap. Below the band gap, transmission dominates with a tiny extinction coefficient. As the band gap energy is approached from below, both *n* and *k* increase with *k* approaches a resonance characterized by one of the oscillators in the Lorentz model. Meanwhile, the refractive index of PMN–PT films reaches a maximum for films deposited at 670 °C. The lowering of refractive index for films deposited at 710 °C may be caused by the loss of PbO. It is well known that PbO would evaporate and escape from the film surface at an elevated post-deposition annealing temperature.[9] In this

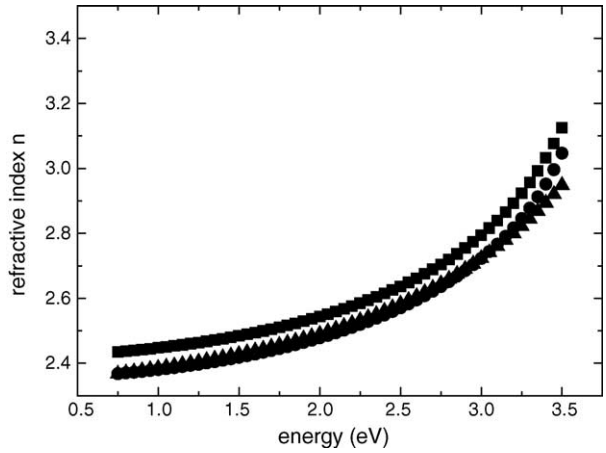

Fig. 4. Refractive indices of PMN–PT films deposited at 630 °C (●), 670 °C (■) and 710 °C (▲).

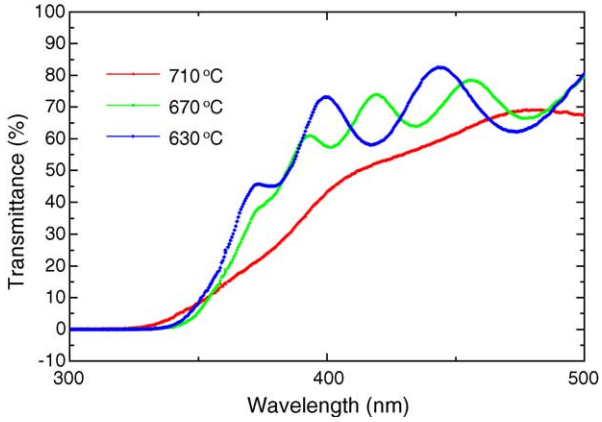

Fig. 6. Transmission spectra of PMN–PT films on MgO substrates with different deposition temperatures.

circumstance, PbO evaporation and grain densification increase the film's porosity and hence locally reduce the density of the film. This reduction of film's density would certainly decrease the refractive index of the film. As a result, the refractive index of the films decreases at higher post-deposition annealing temperatures. Fig. 5 shows the extinction coefficient dispersion curves of the PMN–PT films. According to Fig. 5, the extinction coefficient of PMN–PT film deposited at 710 °C, particularly at higher energy region, is larger than those of the other two films. This larger extinction coefficient may be due to voids caused by PbO evaporation and a larger grain size, resulting in a stronger scattering of light.

As we have mentioned, the optical properties of PMN–PT are dominated by inter-band electronic transitions between the lower lying conduction bands and the upper valence bands of BO_6 octahedra. It is of great interest to investigate the change of the optical band gap of PMN–PT films deposited at different temperatures. The absorption coefficients of the films can be obtained from extinction coefficients using:

$$\alpha = \frac{4\pi}{\lambda}k \tag{2}$$

where α is the absorption coefficient and λ the wavelength. Then, the optical band gap energies of PMN–PT films were deduced from the absorption coefficient α and the energy of the incident light $h\nu$ using Tauc equation:[10]

$$(\alpha h\nu)^2 = B(h\nu - E_g) \tag{3}$$

where B is a constant and E_g the band gap energy. Inset of Fig. 5 shows the dependence of the absorption coefficients $(\alpha h\nu)^2$ on the photon energy for PMN–PT films deposited at 710 °C. By extrapolating the linear portion curve of the curve to zero, the band gap energies obtained for all PMN–PT films deposited at different temperatures are close to ~3.50 eV.

In order to verify the values of the band gap energies of PMN–PT films, optical transmittance measurements were carried out. Fig. 6 shows the transmittance spectra of

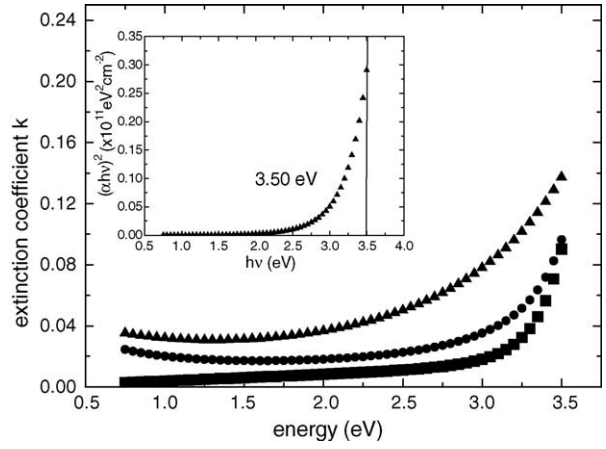

Fig. 5. Extinction coefficients of PMN–PT films deposited at 630 °C (●), 670 °C (■) and 710 °C (▲). Inset shows the dependence of $(\alpha h\nu)^2$ obtained from the fitted extinction coefficients against the photon energy for PMN–PT film deposited at 710 °C.

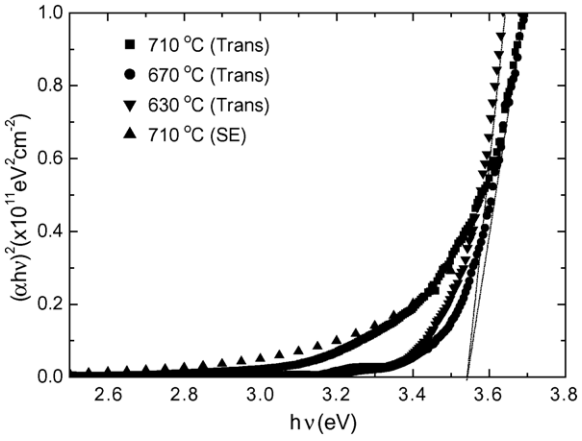

Fig. 7. The dependence of $(\alpha h\nu)^2$ vs. $h\nu$ obtained from the transmission spectra of PMN–PT films on MgO substrates with different deposition temperatures.

PMN–PT films. The transmittance curve of PMN–PT film with 710 °C deposition temperature shows a larger absorption at wavelengths below band gap, which is agreed with the larger extinction coefficient obtained by SE measurements. Fig. 7 shows the dependence of the absorption coefficients $(\alpha h\nu)^2$ on the photon energy obtained from the transmittance spectra. Similarly there is no observable change in the band gap energies as we changed the deposition temperature from 630 to 710 °C. The absorption coefficients $(\alpha h\nu)^2$ for films deposited at 710 °C obtained by SE is also plotted for comparison. We notice that the two sets of absorption coefficients obtained by two different techniques take on similar trend and values. They both indicate that band gap energy of PMN–PT film is not sensitive to deposition temperature.

4. Conclusion

$0.65PbMg_{1/3}Nb_{2/3}O_3$–$0.35PbTiO_3$ (PMN–PT) thin films with different deposition temperatures have been successfully fabricated on (0 0 1)MgO single crystal substrates by PLD. SE was used to characterize the depth-profile, refractive index and extinction coefficient of these films. It is found that the refractive index of PMN–PT films decreases at higher deposition temperature, while its extinction coefficient is larger than those of the other two films. The surface roughness and the film thickness of the films obtained from double-layer Lorentz model are consistent with those measured by SEM and AFM. The transmittance results show that the change in the optical band gap energy of PMN–PT film with deposition temperature is less sensitive than that with composition.

References

1. Xu, Y., *Ferroelectric Materials and Their Applications*. North-Holland, Amsterdam, 1991.
2. Lu, Y. H., Zheng, J. J., Golomb, M. C., Wang, F. L., Jiang, H. and Zhao, J., In-plane electro-optic anisotropy of $(1-x)Pb(Mg_{1/3}Nb_{2/3})O_3$–$xPbTiO_3$ thin films grown on (1 0 0)-cut $LaAlO_3$. *Appl. Phys. Lett.*, 1999, **74**, 3764.
3. Adachi, H., Mitsuyu, T., Yamazaki, O., Wasa, K. and Ferroelectric, $(Pb,La)(Zr,Ti)O_3$ epitaxial thin films on sapphire grown by rf-planar magnetron sputtering. *J. Appl. Phys.*, 1986, **60**, 736.
4. Nagarajan, V., Ganpule, C. S., Nargaraj, B., Aggarwal, S., Alpay, S. P., Roythurd, A. L. *et al.*, Effect of mechanical constraint on the dielectric and piezoelectric behavior of epitaxial $Pb(Mg_{1/3}Nb_{2/3})O_3$(90%)–$PbTiO_3$(10%) relaxor thin films. *Appl. Phys. Lett.*, 1999, **75**, 4183.
5. Tynina, M., Levoska, J., Sternberg, A. and Leppävuori, S., Dielectric properties of pulsed laser deposited films of $PbMg_{1/3}Nb_{2/3}$–$PbTiO_3$ and $PbSc_{1/2}Nb_{1/2}O_3$–$PbTiO_3$ relaxor ferroelectrics. *J. Appl. Phys.*, 1999, **86**, 5179.
6. Stephens, R. E. and Maalitson, I. H., *J. Res. Natl. Bur. Stand.*, 1952, **49**, 249.
7. Mak, C. L., Lai, B., Wong, K. H., Choy, C. L., Mo, D. and Zhang, Y. L., Spectroellipsometric study of sol–gel derived potassium sodium strontium barium niobate films. *J. Appl. Phys.*, 2001, **89**, 4491.
8. Yeung, K. M., Tsang, W. S., Mak, C. L. and Wong, K. H., Optical studies of ZnS:Mn films grown by pulsed laser deposition. *J. Appl. Phys.*, 2002, **92**, 3636.
9. Fox, G. R., Krupanidhi, S. B., More, K. L. and Allard, L. F., Composition/structure/property relations of multi-ion-beam reactive sputtered lead lanthanum titanate thin films. Part I: Composition and structure analysis. *J. Mater. Res.*, 1992, **7**, 3039.
10. Tauc, J. C., *Optical Properties of Solids*. North-Holland, Amsterdam, 1972, p. 372.